Bimetallic Thermochemistry: Perturbations in M-H and M-C Bonds Due to the Presence of M'

G. Gregg Reynolds and Emily A. Carter*

Department of Chemistry and Biochemistry, 405 Hilgard Avenue, Los Angeles, California 90024-1569

Received: October 25, 1993; In Final Form: June 13, 1994®

The effect of perturbing the environment of a transition metal–ligand (M–L) complex by the addition of another metal atom, M', was investigated by ab initio generalized valence bond/correlation-consistent configuration interaction methods. We have examined the properties of low-lying states of Pt–X, Zr–X, and (PtZr)–X, where X = {H, CH_3}. The bonding trends of the transition metal diatomic–ligand complexes have been compared to their monometallic analogs. We find that Zr acts as an electron donor in all the diatomic complexes and that in these complexes the hydride–diatomic bond strengths are increased much more on average than the methyl–diatomic bonds relative to the monometallic complexes. For example, the PtZr–H bond strength is increased by over 14 kcal/mol relative to Zr–H, while the Zr–CH_3 bond strength increases only by 4 kcal/mol in the bimetallic complex. The Pt–ligand bond strengths also both increase upon "alloying" the transition metal, but the magnitude of the changes are more similar—8 kcal/mol for the hydride versus 6 kcal/mol in the methyl complex. We comment on the implications of these results for the potential use of PtZr alloys as dehydrogenation catalysts.

Introduction

It is well-known that industrial catalysts often contain more than one metal; however, questions such as why polymetallic materials have superior catalytic properties compared with monometallic compounds and how to choose the particular metals to combine for the highest activity and selectivity remain unanswered in many cases. Certain Engel–Brewer intermetallic (early–late transition metal) compounds[1] have elicited our interest for their potential use as bimetallic, high-temperature catalysts. The particular subset of these compounds predicted to have special thermal stability combines group 4 (i.e., Ti, Zr, Hf) with the more traditionally catalytic group 9 or 10 (i.e., Co, Rh, Ir, Ni, Pd, Pt) transition metals (TMs). While experimental measurements of the high melting points and energies of atomization for a few compounds of this type have verified the Engel–Brewer stability model phenomenologically, the theoretical underpinning of the Engel–Brewer theory has been challenged recently.[2] Thus, further investigation of these compounds is warranted. Our hypothesis is that such early–late intermetallic compounds might be of use for catalyzing endothermic reactions (which in general must be run at elevated temperatures), precisely because of their thermal integrity and their general resistance to oxidation.[3] In particular, we hypothesize that these compounds may prove especially useful for hydrocarbon dehydrogenation catalysis, due to the propensity of the early transition metals to form strong metal–hydrogen bonds but weaker metal–carbon bonds.[4] This could facilitate selective dehydrogenation by allowing the desired olefin, alkyne, or arene to desorb after formation, also preventing carbidization of the catalyst. Therefore, this study aims to elucidate the chemical reactivity of a model Engel–Brewer compound and, hence, to examine qualitatively its potential as a dehydrogenation catalyst.

The present study centers around the simplest model of a particular bimetallic early–late TM system, namely the diatomic complex PtZr. Wang and Carter[2] first described this cluster theoretically, and this investigation continues their work by characterizing the interaction of the diatomic with the simplest hydrocarbon fragments: hydrogen and methyl radicals. The central idea here is to establish the characteristics of the monometallic–ligand systems for both Pt and Zr and then to examine the changes in the properties of the metal–ligand bond brought about by "alloying" the original metal atom with the other TM of the PtZr diatomic.

Several groups in the past 15 years have investigated the properties of Zr and Pt atoms individually or combined with one of the ligands considered here. The PtH molecule has been examined the most extensively, while to our knowledge $PtCH_3$ has not been studied before the present work. In 1979, Basch and Topiol[5] published bond lengths and dissociation energies for low-lying states of PtH using optimal double configuration[6] wave functions and modified versions of the relativistic effective core potentials (RECPs) of Kahn and co-workers.[7] They predicted ground state of PtH to be $^2\Delta$ with a bond energy of 65.0 kcal/mol and a bond length of 1.470 Å. In 1984, Low and Goddard[8] predicted the bond length in the ground state of PtH to be 1.526 Å and the dissociation energy (DE) to be 51.7 kcal/mol at the GVB-CI level of theory. (GVB-CI is a complete active space (CAS) configuration interaction (CI) calculation, where a full CI within the correlated generalized valence bond (GVB) electron pairs is performed.) In 1986, Poulain et al.[9] used variational and perturbative CI calculations with RECPs to estimate the PtH ground state's bond length to be 1.512 Å and DE to be 59.5 kcal/mol. Rohlfing et al.[10] used fourth-order Moller–Plesset perturbation theory with up to quadruple excitations (MP4 SDTQ) as corrections to unrestricted Hartree–Fock (UHF) wavefunctions on the PtH system utilizing Hay and Wadt's RECP's[11] to obtain a $^2\Delta$ ground-state bond length of 1.561 Å and a DE of 64.3 kcal/mol. Also for PtH, in 1990, Tobisch and Rasch[12] published results using RECPs with multireference single and double excitation CI (MRSDCI) along with perturbative estimates of the full CI energy based on the Langhoff–Davidson approach[13] that predicted the bond length and DE of the $^2\Delta$ state to be 1.534 Å and 70.1 kcal/mol. All of these are fairly consistent with the experimental spectroscopic absorption measurements on PtH which yielded R_e = 1.528 Å[14,15] and DE < 79.3 kcal/mol,[14] though the range in bond energies is rather large (~18 kcal/mol). Finally, recent calculations by Dyall[16] on the low-lying states of Pt atom and PtH using all-electron Dirac–Hartree–Fock calculations, which include explicit spin–orbit effects, demonstrated that spin–orbit splitting is of comparable importance to correlation effects in these systems and that a precise description of the bonding in these complexes necessitates the inclusion of spin–orbit effects. However, the great expense of these calculations in general, the unfeasibility of performing them on a system

® Abstract published in *Advance ACS Abstracts*, July 15, 1994.

0022-3654/94/2098-8144$04.50/0 © 1994 American Chemical Society

as large as ZrPt, and the proximity of our results and previous work using spin-averaged RECPs to J-averaged experimental results shows that the current level of theory is quite adequate in many cases.

The monometallic Zr complexes investigated in this report have been studied by Bauschlicher, Langhoff, and co-workers, who examined a series of both TM methyls[17] and TM hydrides.[18] They predicted the ground state, bond length, and DE for ZrH to be $^2\Delta$, 1.857 Å, and 56.3 kcal/mol, respectively, and those for $ZrCH_3$ to be ^2E, 2.204 Å, and 53.3 kcal/mol, using modified coupled pair functional theory (MCPF)[19] and RECPs.[11] All the above reports also contain some estimates of the atomic splitting of Pt or Zr using the same methods and basis sets as were used to describe the molecules, and some contain other calculated properties of low-lying states of the various species. Thus there is a wealth of calculations to serve as calibration points for this work.

Also of interest is previous research into properties of $ZrPt_x$ clusters. Wang and Carter conducted an extensive study of the low-lying states of the PtZr diatomic and the $ZrPt_3$ cluster[2] using the RECPs and basis sets of Hay and Wadt and CASSCF calculations.[20] Generally, they found that the diatomic and tetratomic were bound quite strongly compared to monometallic clusters ($E_{atomization}$ being at least 101.1 kcal/mol for $ZrPt_3$ and DE = 80.9 kcal/mol for the ground state of PtZr), in agreement with the Engel–Brewer prediction of enhanced stability. However, while charge transfer is significant in these clusters, they found that it occurs in the opposite direction (from Zr to Pt) than what was assumed by Engel and Brewer. Furthermore, Wang and Carter found that d–d bonding, which Engel and Brewer believed to be the key to these complexes' stability, was relatively unimportant in these early–late TM complexes; rather, the intermetallic bonding was strong because of a superposition of ionic and metallic (sp–sp) bonding. The present work is a partial continuation of this previous investigation; here we are determining the properties of hydride and methyl bonds to two of the low-lying states of PtZr using a similar level of theory and will compare our results to those for the single metal atom–ligand interactions.

Theoretical Methods

All the multiconfigurational self-consistent field (MCSCF) calculations performed in this study utilized the GVB2P5 suite of programs developed by Goddard and co-workers.[21] These programs calculate energies and wavefunctions within the generalized valence bond perfect pairing (GVB-PP)[22] theory of electronic structure. In essence, GVB is an MCSCF wave function that is the most general one electron per orbital description, which in its full implementation is very costly. Therefore, typically only those valence electrons involved in bonds or lone pairs are treated within the GVB framework; the rest of the molecule is treated in a restricted Hartree–Fock (RHF) fashion. Also, the "perfect pairing" (GVB-PP) restriction generally is enforced, which imposes orthogonality between correlated electron pairs and requires that the spins of the electrons within a given correlated pair be explicitly singlet coupled.

In the present study, we used a variety of levels of GVB theory to describe the molecules and fragments considered. The two simplest fragments—methyl radical and hydrogen atom—were described by restricted open-shell HF (ROHF) wave functions with C_s and spherical symmetry, respectively. Zr atom was treated at two levels of theory, depending on its spin. The ^5F (s^1d^3) state was treated at the ROHF level; for the ^3F (s^2d^2) state, which has one less orbital (or variational degree of freedom), we correlated the s electrons with an unoccupied p orbital perpendicular to the bond axis to form a GVB(1/2) (GVB description with one correlated pair consisting of two natural orbitals) description of the atom. Treating the triplet and quintet states of the atom at these levels of theory allows both states' wave functions to have the same number of occupied orbitals, as an attempt to remedy any bias toward higher spin states. This more balanced treatment of different spin states extended into molecules formed with the Zr atoms as well; all M–X (M = metal atom or diatomic, X = {CH_3 or H}) complexes were described using one GVB pair consisting of the metal–ligand bonding orbitals along with any GVB pairs used to describe the fragments. Thus, doublet ZrH (derived from ^3F Zr) was described with a GVB(2/4) wave function, quartet $ZrCH_3$ with a GVB(1/2) wave function, and all Pt–X with a GVB(1/2) wave function since the ^3D ground state of Pt atom was calculated at the ROHF level. The states of the PtZr moiety were described using a GVB(4/8) wave function based on the appropriate converged CASSCF wave functions of Wang and Carter.[2] Thus all the metal diatomic–ligand complexes were described using a GVB(5/10) wavefunction, where the extra correlated electron pair is the M–X bond pair.

We followed a systematic method of incorporating electron correlation effects past the MCSCF level. The GVB(N/2N)-PP wave function allows each natural orbital of each pair to be either doubly occupied or unoccupied independent of all other pairs in each configuration included in the MCSCF calculation, and thus it consists of 2^N configurations. The first step after GVB-PP was to use restricted CI (RCI); this allows single occupation of both natural orbitals of each GVB pair (as well as all spin couplings between the open-shell electrons) and thus consists of 3^N configurations.[23,24] At the highest level of correlation considered, we used correlation-consistent CI (CCCI).[24] CCCI is a prescription for obtaining bond dissociation energies that contains excitations from all configurations of a given RCI wave function: it can be most succinctly described as RCI*(SD_{bond} + S_{val}), where SD_{bond} indicates single and double excitations from the GVB pair describing the dissociating bond to all other orbitals and S_{val} indicates single excitations from all valence orbitals to all orbitals. CCCI has been found to be nearly size-consistent and also compares favorably with other CI approaches in predicting particularly single bond strengths, usually coming within experimental error.[24-26] Thus all total and bond energies will be reported at the appropriate GVB-PP, RCI, and CCCI levels of calculation.

We included higher correlation effects in the following way. For RCI, the full RCI space was always used. Thus, for HPtZr, which was first converged self-consistently as a GVB(5/10)-PP wave function, the corresponding RCI calculation involved an RCI(5/10) on the molecule, which upon dissociation correlates with RCI(4/8) and ROHF descriptions of the PtZr and H atom fragments, respectively. For the monometallic complexes, the full CCCI space was used. Thus, for doublet ZrH, the highest level of electron correlation involved a CCCI calculation from the RCI(2/4) multireference space (the RCI consisted of correlation of the Zr 5s pair and the Zr–H bond pair). For the metal diatomic complexes, conducting a CCCI calculation from the full RCI(5/10) space (≥750 000 spin eigenfunctions) for the molecule would have been prohibitively expensive. Thus, we conducted the CCCI calculation for these complexes only from the RCI(1/2) space comprised of the metal diatomic–ligand bond pair. To gaurantee that this calculation was indeed a higher level treatment of correlation effects than the RCI(5/10), all the RCI(5/10) configurations not generated independently in the CCCI expansion were also included in the final CI expansion. The PtZr diatomic molecule calculations can thus be described as CCCI(1/2) + RCI(5/10), where CCCI(1/2) denotes a CCCI from only the RCI(1/2) reference configurations. The corresponding calculations of [dominant*S_{val} + RCI(4/8)] and [HF*S_{val}] were carried out on the dissociated metal diatomic and ligand fragments, respectively. (Dominant refers to the dominant CI reference configuration, the GVB configuration where each GVB pair's bonding natural orbital is doubly occupied.)

The transition metal atoms were represented in general by RECPs and better than double-ζ quality basis sets. For Zr, the Hay–Wadt[11] (8s5p4d) basis was contracted to [4s3p2d] ((8s5p4d)/[4s3p2d]), where the 4s and 4p outermost core electrons are explicitly included. This basis set will be referred to as basis 1 and is the main basis set used for Zr in this work. To test for basis set completion, the Zr and ZrH calculations were repeated with the same RECP but with the basis set augmented (basis 2) with one diffuse d function taken from Bauschlicher and co-workers' basis[18] set (ζ_d = 0.0382). The differences between the predictions of the two basis sets were found to be insignificant.

For Pt, the Hay–Wadt (3s3p3d)/[3s2p2d] basis set was initially used,[11] explicitly including only the 5d and 6s electrons in the calculations. Previous investigations[26,10] have maintained that this basis set and corresponding 10-electron RECP should be adequate for atomic and hyride bond energy calculations conducted at least at the SCF level, but inaccuracies in the predicted PtH bond lengths led us to repeat our calculations with the higher quality 18-electron RECP and corresponding (8s5p3d)/[4s3p2d] basis set of Hay and Wadt. These Pt–H calculations with the 18-electron RECP consistently predicted bond energies which were 7–11 kcal/mol greater and equilibrium bond lengths which were 0.03–0.09 Å shorter than those predicted by the 10-electron RECP. These discrepancies are consistent with those originally found by Rohlfing and co-workers[10] for PtH using the same RECPs and UHF wave functions with MP2 and MP4 energy corrections. We use the 18-electron RECP results for PtH to suggest refinements in our predictions. However, while the two RECPs differ somewhat in their predictions of certain properties, the 10-electron RECPs bond energy predictions are in sufficient agreement with those of previous theoretical and experimental investigations (see discussion of bond lengths, state splittings, and bond energies below) for the purposes of this study. Further investigation of the differences between the predictions of the two RECPs is currently being conducted, in order to ascertain which RECP is more reliable. In the present study, all the calculations used the 10-electron RECP to help reduce their cost; the results of the test calculations on PtH using both RECP's are also presented here: the labels RECP 1 and RECP 2 refer to the 10-electron RECP and 18-electron RECP, respectively.

The carbon atoms were represented by the Dunning-Huzinaga (9s5p)/[3s2p] valence double-ζ (VDZ) basis set,[27] augmented by one d-polarization function (ζ_d = 0.64). For the methyl hydrogens, we used the scaled Dunning–Huzinaga (4s)/[2s] VDZ Gaussian basis set[27] with one p-polarization function (ζ_p = 1.0). For hydrogen atoms directly bonded to a metal atom, a higher quality triple-ζ plus polarization basis set was utilized, namely, the unscaled Huzinaga[27b] (6s)/[3s] with one p-polarization function (ζ_p = 0.6). The contraction of the triple-ζ H basis was achieved by contracting the four tightest primitives into one, leaving the other two primitives uncontracted.

All equilibrium geometries were optimized using analytic gradients[28] of the GVB-PP wave functions. All the geometries were optimized using the smaller basis 1 for Zr and the 10-electron RECP for Pt; the equilibrium bond lengths for PtH were found for both RECPs. The wave functions of the monometallic hydrides were calculated using C_{2v} symmetry; all the other complexes were described in the C_s point group.

Results and Discussion

Atomic state splittings for the two lowest-lying states for Zr atom (^{3}F and ^{5}F) are included along with other total energies for various fragments at various levels of theory in Table 1. These are included as a calibration of the RECPs, the basis sets used, and the various levels of calculation compared to previous results. Further details on the basis sets and RECPs used can be found in earlier work.[2,26] One can see that dynamic correlation is essential for closely reproducing the J-averaged experimental value[29] of $\Delta E(^5F–^3F,Zr)$ = 12.7 kcal/mol: GVB-PP(1/2) with either basis underestimates the stability of the triplet state by 10 kcal/mol. The value improves dramatically, however, once CCCI-types of excitations[23] (RCI(1/2)*$SD_{5s\ pair}$) are included. Then the prediction of the splitting comes to within 1.5 kcal/mol of the experimental value for both basis 1 and 2. Both basis sets' predictions are reasonably close (within 0.6 kcal/mol) to the MCPF prediction by Bauschlicher et al.[17] using better basis sets (ΔE = 13.6 kcal/mol).

TABLE 1

(a) Atomic Fragment Energies

fragment	sym[a]	level[b]	total energy (hartrees)	ΔE[c] (kcal/mol)
Zr Basis 1[d]	^{5}F	HF	–45.980 39	14.2
Zr Basis 1	^{3}F	GVB(1/2)-PP	–45.984 70	11.5
Zr Basis 1	^{3}F	RCI(1/2)	–45.984 70	11.5
Zr Basis 1	^{3}F	RCI(1/2)*S_{val}	–45.989 22	8.7
Zr Basis 1	^{3}F	RCI(1/2)*SD_{5s}	–46.003 08	0.0
Zr Basis 2[d]	^{5}F	HF	–45.980 41	14.2
Zr Basis 2	^{3}F	GVB(1/2)-PP	–45.984 70	11.5
Zr Basis 2	^{3}F	RCI(1/2)	–45.984 70	11.5
Zr Basis 2	^{3}F	RCI(1/2)*S_{val}	–45.989 24	8.7
Zr Basis 2	^{3}F	RCI(1/2)*SD_{5s}	–46.003 10	0.0
Pt RECP 1[e]	^{3}D	HF	–26.238 10	1.2
Pt RECP 1	^{3}D	HF*S_{val}	–26.240 09	0.0
Pt RECP 2[e]	^{3}D	HF	–118.226 48	1.0
Pt RECP 2	^{3}D	HF*S_{val}	–118.228 16	0.0
H	^{2}S	HF (6s/[3s])	–0.4999 4	0.0

(b) Molecular Fragment Energies

fragment	sym[f]	level[b]	total energy (hartrees)	ΔE[c] (kcal/mol)
CH_3	^{2}A″	HF	–39.567 53	5.7
CH_3	^{2}A″	HF*S_{val}	–39.576 61	0.0
PtZr RECP 1[e]	^{3}A′	GVB(4/8) for Zr–X	–72.281 82	21.9
PtZr RECP 1	^{3}A′	RCI(4/8) for Zr–X	–72.313 99	1.7
PtZr RECP 1	^{3}A′	dominant*S_{val}+RCI(4/8)	–72.316 74	0.0
PtZr RECP 1	^{3}A″	GVB(4/8) for Pt–X	–72.273 20	27.3
PtZr RECP 1	^{3}A″	RCI(4/8) for Pt–X	–72.288 02	16.3
PtZr RECP 1	^{3}A″	dominant*S_{val}+RCI(4/8)	–72.288 80	15.8

[a] Atom calculations used spherical symmetry. [b] GVB-PP refers to generalized valence bond with the perfect pairing and the strong orthogonality restriction. RCI refers to a restricted configuration interaction calculation from the GVB wave function. CCCI refers to correlation consistent configuration interaction. S_{val} refers to excitations from valence orbitals to all other orbitals. Dominant refers to the configuration in which the bonding natural orbitals of each GVB pair are doubly occupied. See Theoretical Methods for more details. [c] State splittings in kcal/mol. [d] Basis 1 refers to the standard Hay and Wadt basis set (8s5p4d)/[4s3p2d] for Zr's 12-electron RECP.[11] Basis 2 is basis 1 supplemented by a diffuse d function (ζ_d = 0.0382[18]). [e] RECPs 1 and 2 are the 10- and 18-electron Pt RECPs, respectively.[11] [f] All molecular fragment calculations used C_s symmetry.

Table 2 contains predicted equilibrium bond lengths of the low-lying monometallic hydride states listed in decreasing order of their total energies, while Figure 1 graphically depicts the bond lengths and angles for the methyl complexes and PtZr diatomic hydrides. For ZrH and $ZrCH_3$, the bond lengths of the quartet states are generally larger than those of the doublet states, as one might expect from repulsions from the extra open shell d orbitals. Bond pair-d orbital repulsions also lead to a slight decrease in the HCH angles in the quartet versus doublet states of $ZrCH_3$. Finally, the contraction of the radial extent of the d orbitals going from the early second row TM to the late third row TM leads to shorter metal–ligand bonds in PtH and $PtCH_3$ and to larger HCH angles in $PtCH_3$ due to decreased bond pair-d orbital repulsions, compared to the analogous Zr complexes.

The predicted equilibrium structures are generally in good agreement with previous calculations. The bond lengths for the appropriate states of ZrH are close to those predicted by the

TABLE 2: Equilibrium Geometries of ZrH, PtH, and CH_3 at the GVB-PP Level

molecule	state	occupation of open-shell d orbitals	R_e (Å)
ZrH	$^4\Delta$	$\delta\pi\bar{\pi}$	2.021
	$^2\Sigma^+$	σ	1.931
	$^4\Pi$	$\pi\delta\delta$	2.023
	$^4\Sigma^-$	$\pi\bar{\pi}\sigma$	1.931
	$^2\Pi$	$\bar{\pi}$	1.838
	$^4\Sigma^-$	$\delta\delta\sigma$	1.922
	$^2\Delta$	δ	1.852
PtH RECP 1[a]	$^2\Pi$	π	1.701
	$^2\Sigma^+$	σ	1.588
	$^2\Delta$	δ	1.616
PtH RECP 2[a]	$^2\Pi$	π	1.612
	$^2\Sigma^+$	σ	1.558
	$^2\Delta$	δ	1.555

fragment	R_e (Å)	θ (deg)
CH_3 $^2A''$	1.074	120.0

[a] See Table 1a, footnote *e*.

MCPF calculations of Langhoff et al.,[18] e.g., 1.852 Å for our ZrH ground state versus 1.857 Å for theirs. The agreement with Bauschlicher et al.'s[17] geometry optimized at a higher level treatment of electron correlation (MCPF) for $ZrCH_3$ is also good. Bauschlicher predicts the Zr–C–H angle to be 109.8° for the ^2E state. For our two components of this state in C_s symmetry, the average bond angle is 109.8° as well. Also our average equilibrium bond Zr–C length of 2.237 Å is only 1.4% different from their prediction of 2.205 Å. The bond lengths for the PtH species using RECP 1 all appear to be somewhat longer than other studies have predicted, 1.616 Å for our $^2\Delta$ state versus 1.5 Å as an approximate average of all other predictions, but they follow the same general ordering as those from the MP4-SDTQ calculations of Rohlfing et al.[10] The bond lengths predicted by calculations using RECP 2 are uniformly shorter and agree much more closely with experiment and theory. The prediction of 1.555 Å for the $^2\Delta$ PtH bond length is only 2% different from the experimental value of 1.528 Å, and all the bond lengths given by RECP 2 agree to within 1% with those predicted by the UHF calculations of Rohlfing and co-workers[10] using the same RECP. Thus, use of RECP 1 in other calculations may well result in overestimation of Pt bond lengths by less than 0.1 Å. No calculations of which we are aware have been reported for $PtCH_3$.

The geometric trends found for the monometallic complexes also continue in the metal diatomic–ligand complexes: the Zr–ligand bonds are significantly longer than the Pt–ligand bonds and the HCH angles expand from $PtZrCH_3$ to $ZrPtCH_3$. The geometries of the metal diatomic–ligand complexes are also sensitive to the placement of the ligand: The metal–metal bonds are longer and the metal–metal–ligand bond angle is much smaller when Pt bonds to the ligand. For example, the optimized structure for ZrPt–H has a bond angle of only 86.3°. Figure 2 shows the GVB one-electron orbitals describing the Pt–H bond pair. The small bond angle can be attributed in part to an electrostatic attraction between the Pt–H bond and the positively charged Zr atom, as evidenced by the slight delocalization of the Pt–H bonding electrons toward the Zr atom. This can be thought of as an "agostic" interaction, often seen in early transition metal complexes. By contrast, PtZrH has the opposite electrostatic forces at play: the relatively negative Pt repels the likewise negatively charged H atom, leading to a bond angle of 135.1°. This also makes sense from an orbital overlap point of view. As Figure 3 shows, the Zr–H bond is comprised of an H 1s orbital and a 4d orbital on Zr that has its maximum at an angle of 135° from the metal diatomic bond. The $PtZrCH_3$ Pt–Zr–C bond angles in both the cis and trans conformers are larger than that of PtZrH, due to the greater steric repulsions of the CH_3 ligand (see Figures 1 and 4). The Zr–Pt–C bond angle in $ZrPtCH_3$,

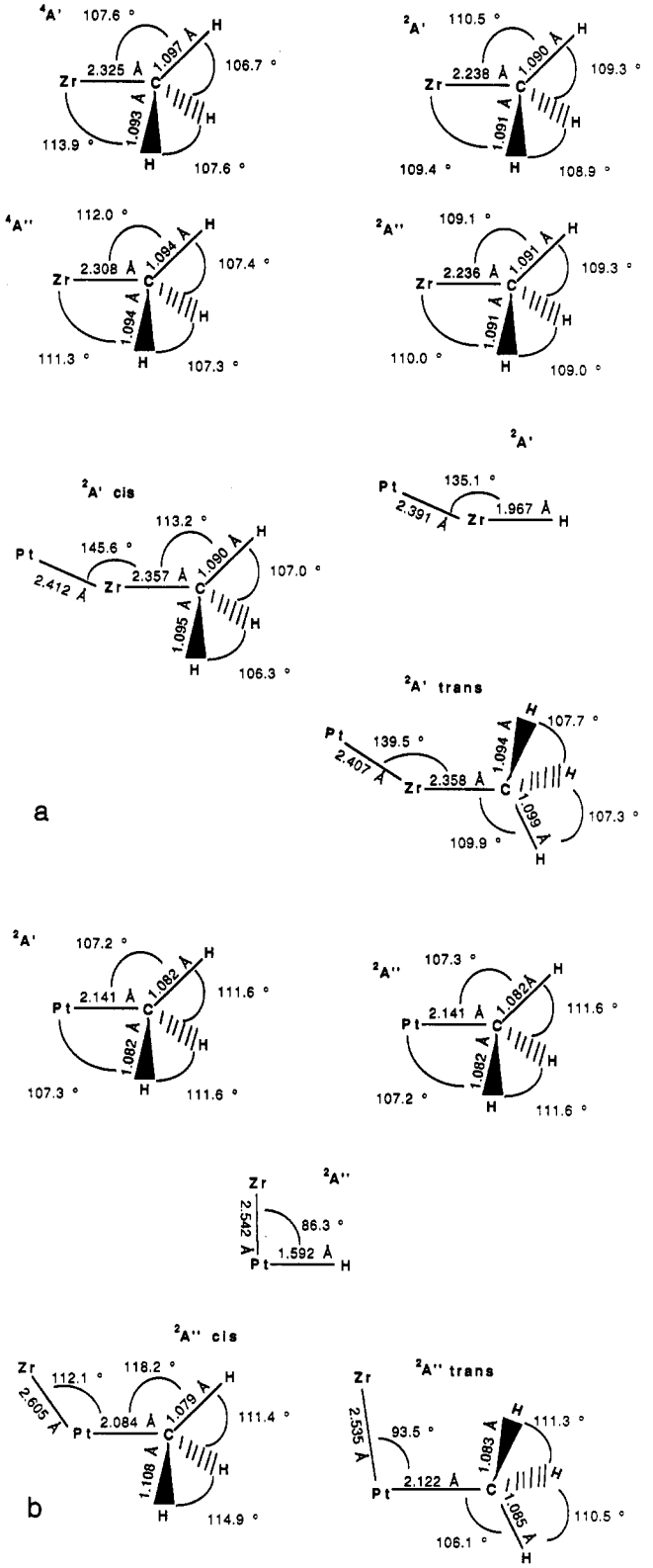

Figure 1. Optimized structures of (a) Zr-bonded and (b) Pt-bonded complexes obtained via GVB-PP analytic gradients.

however, is much smaller at 112.1°, reminiscent of the diatomic–ligand bond angle in ZrPtH. Figure 5 shows the GVB orbitals for the Pt-CH_3 bond where we see that the methyl H atoms may have a slight agostic interaction with the positively charged Zr atom, favoring a small ZrPtC angle. In general, the geometries of the trans and cis conformers of the TM diatomic–methyl complexes are similar. The main difference is that the metal diatomic–C and X–C–H (where X is the TM atom to which the methyl group is bonded and H is the in-plane hydrogen) bond

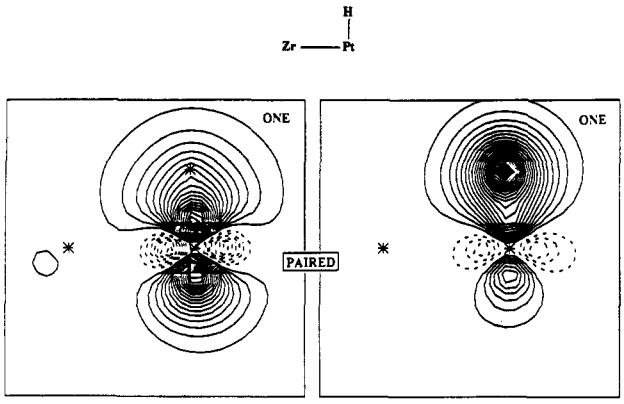

Figure 2. GVB-PP one-electron orbitals for the Pt–H σ bond of ZrPtH. The contours from –0.50 to 0.50 amplitude are plotted in intervals of 0.02. Solid lines indicate positive amplitudes while dashed lines indicate negative amplitudes. The positions of the nuclei are indicated in the plots by asterisks; pictures above the plots show the respective identities of the atoms. The same contour ranges and intervals and plotting conventions are used in all the plots.

angles contract slightly upon going from the cis to the trans arrangement of the metal diatomic–C–H moiety. This is presumably due to the ability of the trans species to increase bonding orbital overlap by contracting these bond angles once the steric interaction between the in-plane hydrogen and the TM diatomic is removed. This is a minor point though: The dominant geometrical difference between the Zr-bound ligands and the Pt-bound ligands is the smaller metal diatomic-ligand bond angles for the Pt-bonded complexes, due to the electrostatic ("agostic") attraction between the Zr atom and the ligand.

Table 3 displays GVB-PP, RCI, and CCCI electronic state splittings for the Zr (Table 3a) and Pt (Table 3b) hydrides and methyls. On the basis of these tables, the $^2\Delta$ state of ZrH, the $^2\Delta$ state of PtH, the $^4A''$ state of $ZrCH_3$, and the ^2E state of $PtCH_3$ (actually both of the monometallic-methyl ground states are projections into C_s of one of two degenerate components of the E state in C_{3v} symmetry) are predicted to be the ground states of each of these monometallic species.

Our predicted ordering for the low-lying states of the monometallic complexes is in general agreement with published results. The biggest discrepancy occurs in the comparison to the predictions of Bauschlicher et al.,[17] who found the ground state of $ZrCH_3$ to be of ^2E symmetry in the C_{3v} point group. In Table 3b, our prediction for the $ZrCH_3$ ground state is $^4A''$ within the abelian C_s point group. The disagreement may not be very significant, however. All the doublet states and quartet states of $ZrCH_3$ are within 5 kcal/mol of one another; the two doublet states are separated by only 0.5 kcal/mol and are an average of 3.0 kcal/mol higher in energy than the $^4A''$ state, while the second quartet component is 4.7 kcal/mol higher in energy than the ground state. Thus, the ordering of the lowest-lying quartet and doublet states within the full symmetry group of the molecule may not be quite as clear as in the present case. Also, the properties of both our doublet $ZrCH_3$ states (see the discussions of geometries above and of bond energies and Mulliken electron populations below) are in agreement with those predicted for the ^2E ground state by Bauschlicher and co-workers.[17] Langhoff et al.[18] found that the $^2\Delta$ state of ZrH is the ground state at the MCPF and coupled pair functional (CPF) levels of theory in agreement with our prediction for both basis sets. Note that the largest discrepancy between the two sets of state splittings is less than 1.1 kcal/mol. The ordering of the states is the same for both basis sets except that two low-lying states, $^2\Pi$ and $^4\Sigma^-_{\sigma\pi\pi}$ (which are within 0.5 kcal/mol of one another), are reversed. This might be a problem in definitively assigning the low-lying states of Zr compounds; however, it does not change the qualitative picture or affect the assignment of the ground state. Thus, we conclude that the use of the smaller basis set will not adversely affect our ability to assign ground states. The ordering of the states of PtH with either RECP is in good agreement with that of Rohlfing et al.[10] They designated the $^2\Pi$ state to be ~15.7 kcal/mol above the $^2\Delta$ state, within 0.5 kcal/mol of the assignments of either RECP. By contrast, their relative ordering of the $^2\Sigma^+$ and $^2\Delta$ states is less clear: Two different RECPs predict the energy gap to be the same size, 3.7 kcal/mol, but in opposite directions of one another. In our calculations the 10-electron RECP predicts the two states to be degenerate at the CCCI level, the while higher quality RECP predicts that the $^2\Delta$ state lies 2.8 kcal/mol lower at the CCCI level, within 1.0 kcal/mol of their prediction. In sum, agreement between our current predictions for the ordering of the states of ZrX (X = H, CH_3) and PtH with previous high-quality ab initio calculations suggests that our new predictions for $PtCH_3$ should be reasonably accurate. Finally, we note that in both $ZrPtCH_3$ and $PtZrCH_3$, the trans conformer is slightly lower in total energy than the cis species (0.9 kcal/mol for $PtZrCH_3$ and 2.8 kcal/mol for $ZrPtCH_3$). Again as mentioned above in comparing geometries, the increase in stability of the trans TM diatomic–methyl species results from lessened steric interactions between the metal diatomic moiety and the in-plane hydrogen and from improved orbital overlap gained by the trans species' equilibrium geometries.

Listings of the overall molecular charge distributions as estimated by Mulliken electron populations for the various complexes at the GVB-PP level are located in Table 4. For the monometallic ligand complexes, the results are mostly as expected: Partial charge transfer occurs from the metal atom to the hydrogen in all the hydrides except PtH, where the charge transfer is minimal (<0.1e), consistent with the greater electronegativity of Pt compared to Zr. We also see that the charge transfer for the ZrH states is insensitive to the addition of a diffuse function of Zr (basis 2 in Table 4a). The two RECPs for Pt differ in their predictions of the direction of charge transfer in the $^2\Sigma^+$ and $^2\Delta$ states of PtH, with RECP 1 predicting a small transfer to Pt and RECP 2 predicting a slight transfer to H, but both predict the magnitude of charge transferred to be small. In the monometallic methyls, one finds substantial transfer of electrons from both the hydrogen and the metal atoms to the carbon atom. Generally, Zr is a better charge donor in all of these complexes, consistently losing between 0.25 and 0.5 e, whereas the charge transfer to or from Pt is rather minimal, again consistent with their relative electronegativities. In the metal diatomic–ligand complexes, an obvious trend emerges: in all of the complexes Zr acts as an electron donor and Pt as an electron acceptor. In PtZrH, Zr donates a whole electron: Pt acquires a partial negative charge of –0.74 e and H takes on a partial charge of –0.24 e. For both conformers of $PtZrCH_3$, Zr acquires a positive charge of ~1.24 e, donating ~0.75 e to Pt and ~0.5 e to C. For those complexes of the diatomic where the ligand is bonded to Pt, the electron donation of Zr is somewhat less. In ZrPtH, Zr takes on a partial positive charge of 0.54 e. Pt liberates electron density from both Zr and H, to acquire a partial negative charge of –0.66 e. In both conformers of $ZrPtCH_3$, Zr again loses ~0.5 e to Pt. Thus in all the metal diatomic–ligand complexes, Pt acquires an excess of 0.5–0.75 e, the ligands remain close to what they were in the corresponding monometallic complexes, and Zr donates the appropriate electron density.

Metal and ligand bonding orbital hybridizations as estimated by GVB-PP Mulliken electron populations are located in Table 5. For the monometallic hydrides, we predict the following trends. In ZrH, the Zr bonding orbital has approximately 20% p character on average. The quartet states without dσ singly-occupied orbitals have much more s character in the bond (50–55%) than the two $^4\Sigma^-$ states (33%) and concomitantly less d character (~30% compared to ~45%). The doublet ZrH states all have only a small s contribution to the bond, approximately 10%, and high

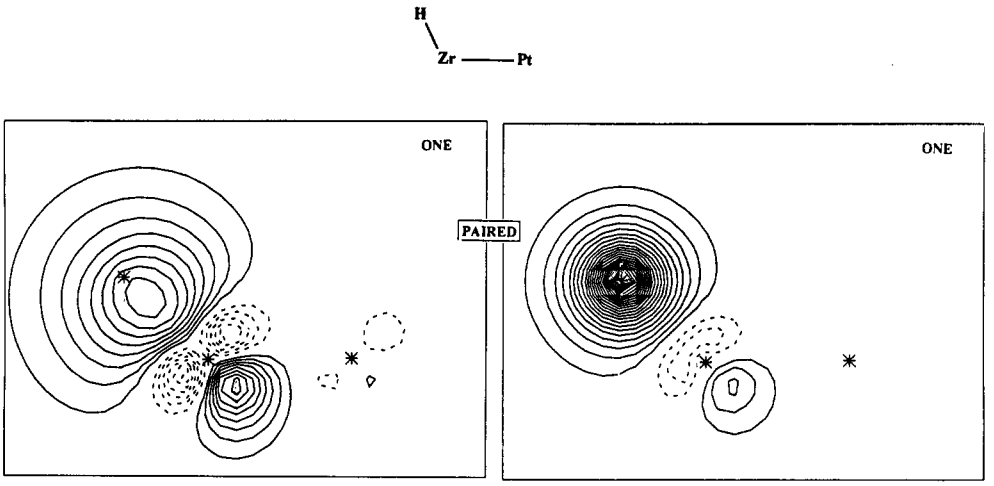

Figure 3. GVB-PP one-electron orbitals for the Zr–H σ bond of PtZrH.

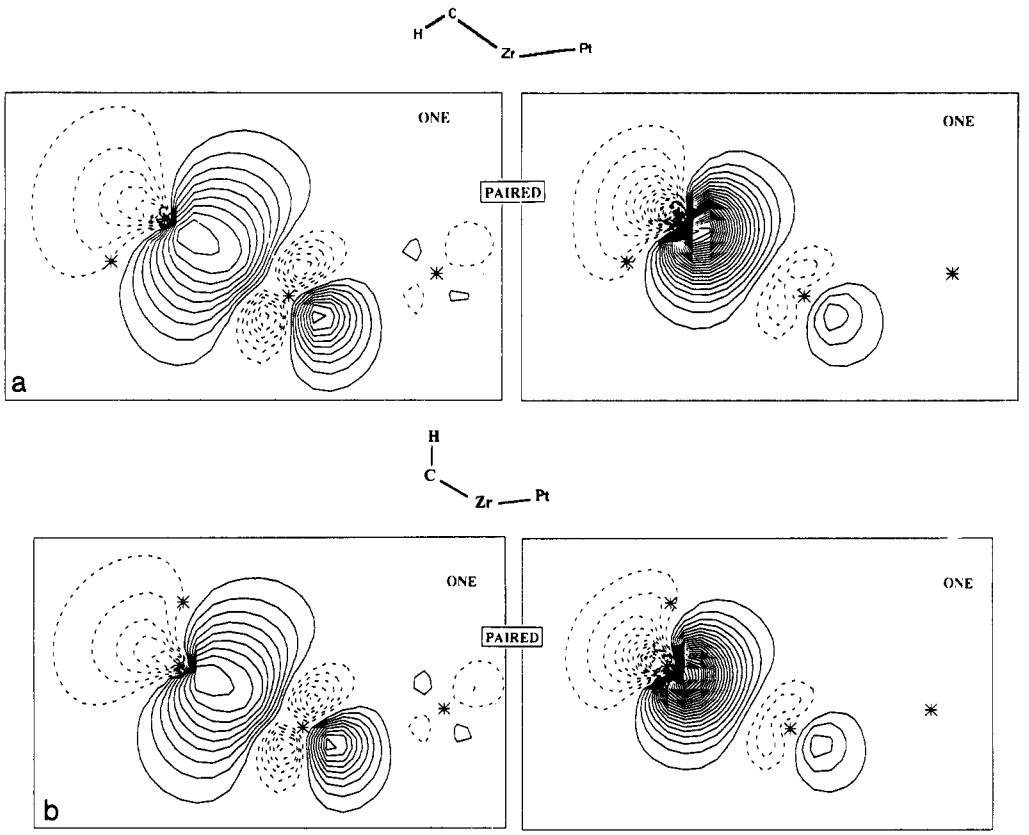

Figure 4. GVB-PP one-electron orbitals for the Zr–C σ bond of the (a) trans and (b) cis conformers of $PtZrCH_3$.

d character (65–75%) due to the double occupation of the 5s orbital in the Zr fragment from which they were formed. Consistent with the discussion of total electron populations on the atoms above, the populations also show that Zr donates a significant amount of charge to H within the bond pair. Although not shown, the hybridization of Zr is not affected by the addition of a diffuse d function (basis 2). In PtH, the bonds are mainly sd hybrids with less than 10% p character. The distribution between s and d character depends on the state and there is some variance between the predictions of the two RECPs. Using RECP 1, the $^2\Pi$ state has more s character (60%) than d (33%), but the $^2\Sigma^+$ and $^2\Delta$ states have just the opposite. With RECP 2, the s (49%) and d (46%) characters of the PtH bond in the $^2\Pi$ state are nearly equal; the s–d hybridizations of the other states' bonds are basically identical to those predicted by RECP 1. In all the states of PtH, the charge within the bond pair resides more on Pt (52–60%) than on H, using RECP 1. Calculations using RECP 2 predict somewhat more covalent bonds, with Pt having 50–54% of the charge within the bond. For the metal diatomic hydrides, the story is similar to that of the monometallics. In PtZrH, the metal bonding orbital has appreciable, nearly equal amounts of s, p, and d character on Zr. In ZrPtH, the metal bonding orbital is basically an sd hybrid with 70% d character, similar to the monometallic PtH in either the $^2\Delta$ or $^2\Sigma^+$ states. Again the charge-transfer characteristics are similar to the monometallic cases, with PtZrH donating much more electron density to the hydrogen ligand than ZrPtH. Comparison of the GVB orbital plots in Figures 2 and 3 also shows that the ZrH bond in Figure 3 involves much greater charge donation (toward H) than the PtH bond in Figure 2.

For the methyl complexes, the hybridization trends are as follows. The carbon atoms generally have much more p character (70–90%) than s character (10–30%), roughly sp^3 hybrids as expected. The metal bonding orbitals all have high d character

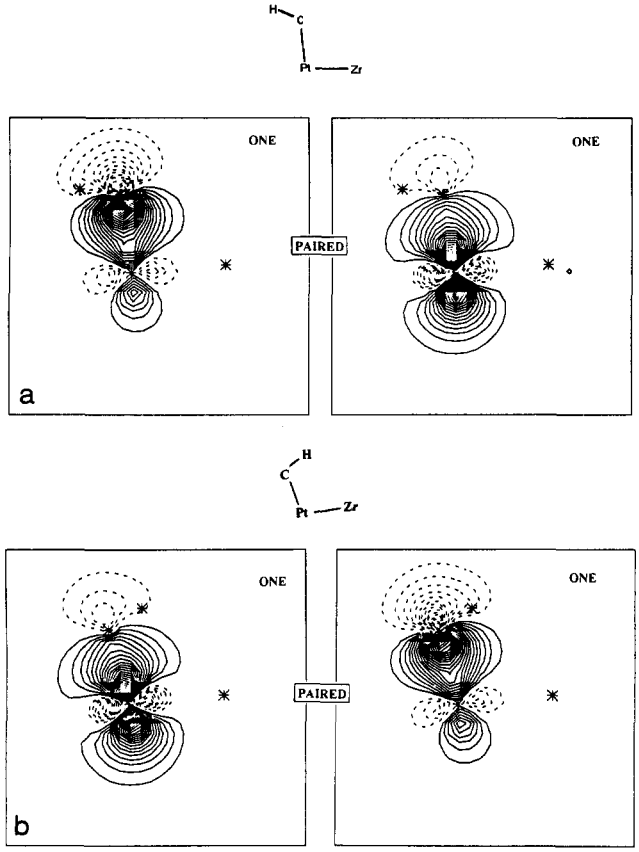

Figure 5. GVB-PP one-electron orbitals for the Pt–C σ bond of the (a) trans and (b) cis conformers of $ZrPtCH_3$.

(55–85%) and low p character (<20%). In $ZrCH_3$, the quartet states have more s character (30%) than the doublet states (10%) and concomitantly less d character (60% and 80%, respectively), as with ZrH and for the same reasons given above. The bonding orbital Mulliken electron populations for the doublet states of $ZrCH_3$ are in general agreement with those of Bauschlicher and co-workers[17] for their ground ^2E state. The predictions of the total percentage of the charge within the bond residing on the metal atom are quite close: 34% in the present study compared with 32% predicted by Bauschlicher et al. The decomposition of this into the populations of the valence s, p, and d orbitals are slightly different. We predict slightly higher d character (~30% total, i.e., 84% of 35%) and lower s/p character (~6%) than Bauschlicher (22% and 9%, respectively). Again, Zr generally loses bonding electron density to C, while Pt gains it in both the monometallic and metal diatomic complexes.

In Table 6, we present the bond energies of the various mono- and bimetallic complexes. There are several trends in the bond strengths that can be isolated for the monometallic ligand systems. We discuss first the more complicated situation of the bond energies for H and CH_3 bound to Zr. There are two atomic asymptotes for the monometallic Zr complexes: the ^3F ground state of Zr resulting from the $5s^24d^2$ valence electron configuration and the ^5F excited state of Zr derived from the $5s^14d^3$ valence electron occupation. The quartet states of monometallic Zr complexes thus have extra promotional costs (14.2 kcal/mol at the CCCI level for basis 1; see Table 1a) to excite the ground-state Zr atom to the quintet state and different exchange losses[30] upon bond formation relative to the doublet states. Since H and CH_3 bond only to the ground ^2D state of Pt atom, promotional costs are not incurred and therefore we need only consider adiabatic bond strengths for Pt complexes.

To help resolve these different promotional and exchange energy effects, we have tabulated the adiabatic, diabatic, and intrinsic bond energies for the various monometallic Zr complexes in Table

TABLE 3

(a) State Splittings and Total Energies at Various Levels of Calculation for Zr and Pt Hydrides

molecule	state[a]	occupation[b]	$\Delta E_{GVB\text{-}PP}$[c,d] (kcal/mol)	ΔE_{RCI}[c,d] (kcal/mol)	ΔE_{CCCI}[c,d] (kcal/mol)
ZrH basis 1[e]	$^4\Delta$	$\delta\pi\bar{\pi}$	18.35	17.92	19.82
	$^2\Sigma^+$	σ	39.30	39.47	9.42
	$^4\Pi$	$\pi\delta\delta$	26.95	26.79	8.07
	$^4\Sigma^-$	$\sigma\pi\bar{\pi}$	4.72	4.60	5.81
	$^2\Pi$	$\bar{\pi}$	10.26	10.22	5.36
	$^4\Sigma^-$	$\sigma\delta\delta$	0.00	0.00	0.74
	$^2\Delta$	δ	2.77[f]	2.82[f]	0.00[f]
ZrH basis 2[e]	$^4\Delta$	$\delta\pi\bar{\pi}$	18.33	17.89	20.89
	$^2\Sigma^+$	σ	39.28	39.45	10.23
	$^4\Pi$	$\pi\delta\delta$	26.97	26.80	9.10
	$^2\Pi$	$\bar{\pi}$	10.21	10.16	6.06
	$^4\Sigma^-$	$\sigma\pi\bar{\pi}$	4.68	4.55	5.91
	$^4\Sigma^-$	$\sigma\delta\delta$	0.00	0.00	1.57
	$^2\Delta$	δ	2.72[f]	2.77[f]	0.00[f]
PtH RECP 1[g]	$^2\Pi$	π	15.2	14.5	16.2
	$^2\Sigma^+$	σ	1.6	0.4	0.0
	$^2\Delta$	δ	0.0[f]	0.0[f]	0.0[f]
PtH RECP 2[g]	$^2\Pi$	π	14.6	14.3	15.5
	$^2\Sigma^+$	σ	4.2	3.2	2.8
	$^2\Delta$	δ	0.0[f]	0.0[f]	0.0[f]

(b) State Splittings and Total Energies at Various Levels of Calculation for Zr and Pt Methyls

molecule	state[a]	$\Delta E_{GVB\text{-}PP}$[b,c] (kcal/mol)	ΔE_{RCI}[b,c] (kcal/mol)	ΔE_{CCCI}[b,c] (kcal/mol)
$ZrCH_3$	$^4A'$	4.7	4.7	4.7
	$^2A'$	4.8	4.9	3.2
	$^2A''$	5.7	5.8	2.7
	$^4A''$	0.0[h]	0.0[h]	0.0[h]
$PtZrCH_3$ RECP 1[d]	$^2A'$(cis)	0.8	0.9	0.9
$PtZrCH_3$ RECP 1	$^2A'$(trans)	0.0[h]	0.0[h]	0.0[h]
$ZrPtCH_3$ RECP 1	$^2A''$(cis)	2.4	3.0	2.8
$ZrPtCH_3$ RECP 1	$^2A''$(trans)	0.0[h]	0.0[h]	0.0[h]

[a] $C_{\infty v}$ symmetry was used for linear hydrides. All other molecules were represented in C_s symmetry. [b] A list of singly occupied d orbitals in the final wave function: $\sigma = d_{z^2}$, $\pi = d_{xz}$, $\bar{\pi} = d_{yz}$, $\delta = d_{x^2-y^2}$, $\delta = d_{xy}$. [c] See Table 1, footnote *b*. [d] The difference of energy in kcal/mol between a given state of a molecule and the ground state for that molecule at the indicated level. [e,g] See footnotes *d* and *e* of Table 1a. [f] The total energies (in hartrees) of the ground states at the GVB-PP, RCI, and CCCI levels of calculation of the various hydrides are as follows: $^2\Delta$ ZrH (basis 1) –46.551 46, –46.551 67, –46.570 58; $^2\Delta$ ZrH (basis 2) –46.551 58, –46.551 79, –46.571 96; $^2A'$ PtZrH –72.875 15, –72.905 21, –72.920 97; $^2\Delta$ PtH (RECP 1) –26.818 52, –26.818 56, –26.841 80; $^2\Delta$ PtH (RECP 2) –118.822 61, –118.822 80, –118.845 37; $^2A''$ ZrPtH –72.854 52, –72.882 10, –72.902 71. [h] The total energies (in hartrees) at the GVB-PP, RCI, and CCCI levels of calculation of the ground states of the various methyls are as follows: $^4A''$ $ZrCH_3$ –85.612 60, –85.612 97, –85.646 36; ^2E $PtCH_3$ –65.863 63, –65.863 70, –65.898 92; $^2A'$ $PtZrCH_3$ –111.925 35, –111.954 04, –111.983 58; $^2A''$ $ZrPtCH_3$ –111.897 89, –111.926 22, –111.956 69.

7. *Adiabatic dissociation* refers to allowing the fragments to relax electronically and geometrically to their equilibrium ground states, whereas with *diabatic dissociation*, we consider the case where the fragments are allowed to relax geometrically, but not electronically. For example, $^4\Delta$ ZrH diabatically dissociates to ^5F Zr even though ^3F is the ground state of Zr atom, and the diabatic bond strength is 14.2 kcal/mol stronger than the adiabatic one. Finally, for *intrinsic bond strengths*, the exchange losses of the atomic asymptote upon bonding are calculated and added to the diabatic bond energy to obtain an exchangeless, promotionless bond energy. The intrinsic bond energy is meant to give a feel for the bond energy trends simply as a function of overlap between the metal and ligand orbitals with all other energetic factors (exchange/promotion) removed. For the ^5F state ($5s^14d^3$), assuming the ligand bonds primarily to the metal s electron, the exchange loss upon single bond formation is $1.5K_{sd}$; the corresponding exchange loss for the ^3F state ($5s^24d^2$) is $0.5K_{dd}$, assuming the ligand bonds primarily to the metal d electron (K_{sd}

TABLE 4

(a) Total Mulliken Populations on Atoms for Low-Lying States of Zr and Pt Hydrides

molecule	Pt[a]	Zr[b]	H1[c]
ZrH basis 1[d]			
$^4\Delta$		11.75	1.25
$^2\Sigma^+$		11.79	1.21
$^4\Pi$		11.74	1.26
$^4\Sigma^-$		11.77	1.23
$^2\Pi$		11.82	1.18
$^4\Sigma^-$		11.77	1.23
$^2\Delta$		11.82	1.18
ZrH basis 2[d]			
$^4\Delta$		11.77	1.23
$^2\Sigma^+$		11.81	1.19
$^4\Pi$		11.76	1.24
$^2\Pi$		11.82	1.18
$^4\Sigma^-$		11.78	1.22
$^4\Sigma^-$		11.78	1.22
$^2\Delta$		11.83	1.17
PtZrH			
$^2A'$ RECP 1[e]	10.74	11.02	1.24
PtH			
$^2\Pi$ RECP 1	9.98		1.02
$^2\Sigma^+$ RECP 1	10.09		0.91
$^2\Delta$ RECP 1	10.06		0.94
$^2\Pi$ RECP 2[e]	17.95		1.05
$^2\Sigma^+$ RECP 2	17.96		1.04
$^2\Delta$ RECP 2	17.97		1.03
ZrPtH			
$^2A''$ RECP 1	10.66	11.46	0.89

(b) Total Mulliken Populations on Atoms for Low-Lying States of Zr and Pt Methyls

molecule	Pt[a]	Zr[b]	C	H1[c]	H2/H3[f]
$ZrCH_3$ basis 1[d]					
$^4A'$		11.50	6.91	0.87	0.86
$^2A'$		11.63	6.86	0.84	0.84
$^2A''$		11.63	6.86	0.84	0.83
$^4A''$		11.51	6.91	0.86	0.86
$PtZrCH_3$					
$^2A'$(cis) RECP 1[e]	10.74	10.76	6.95	0.83	0.86
$^2A'$(trans) RECP 1	10.75	10.77	6.93	0.86	0.84
$PtCH_3$					
$^2A'$ RECP 1	9.92		6.54	0.85	0.85
$ZrPtCH_3$					
$^2A''$(cis) RECP 1	10.47	11.51	6.46	0.87	0.85
$^2A''$(trans) RECP 1	10.46	11.49	6.49	0.86	0.85

[a] Within the RECP approximation, a neutral Pt atom has 10 electrons with RECP 1 or 18 electrons with RECP 2. [b] Within the RECP approximation, a neutral Zr atom has 12 electrons. [c] H1 is the hydride hydrogen in hydrides and the in-plane hydrogen for methyls (all done in C_s symmetry). [d,e] See Table 1a, footnotes *d*, *e*. [f] H2/H3 are the out of plane methyl hydrogens constrained to be identical by symmetry.

TABLE 5

(a) Metal-Ligand Bonding Orbital Hybridizations for Zr and Pt Hydrides[a]

	metal atom[b]				hydrogen atom		
	s%	p%	d%	total%[c]	s%	p%	total%[c]
ZrH basis 1[d]							
$^4\Delta$	55	19	26	38	100	0	62
$^2\Sigma^+$	13	24	64	46	100	0	54
$^4\Pi$	50	18	32	37	100	0	63
$^4\Sigma^-$	34	24	42	39	100	0	61
$^2\Pi$	11	18	71	45	100	0	55
$^4\Sigma^-$	33	17	50	40	100	0	60
$^2\Delta$	11	17	72	45	100	0	55
PtZrH RECP 1[e]							
$^2A'$	29	31	41	38	99	1	62
PtH RECP 1							
$^2\Pi$	60	6	33	52	100	0	48
$^2\Sigma^+$	34	6	61	57	100	0	43
$^2\Delta$	38	5	57	58	100	0	42
PtH RECP 2[e]							
$^2\Pi$	49	5	46	51	99	1	49
$^2\Sigma^+$	35	5	60	50	99	1	50
$^2\Delta$	33	4	63	54	100	0	46
ZrPtH RECP 1							
$^2A''$	25	8	68	60	100	0	40

(b) Metal–Ligand Bonding Orbital Hybridizations for Zr and Pt Methyls[a]

	metal atom[b]				carbon atom			
	s%	p%	d%	total%[c]	s%	p%	d%	total%[c]
$ZrCH_3$ basis 1[d]								
$^4A'$	27	11	62	26	26	73	0	76
$^2A'$	9	8	83	34	22	78	0	66
$^2A''$	7	8	84	35	22	78	0	66
$^4A''$	26	10	64	26	26	74	0	75
$PtZrCH_3$ RECP 1[e]								
$^2A'$(cis)	26	19	55	25	29	71	0	78
$^2A'$(trans)	26	18	56	25	28	72	0	77
$PtCH_3$ RECP 1								
$^2A'$	38	2	60	52	12	87	1	47
$ZrPtCH_3$ RECP 1								
$^2A''$(cis)	23	3	73	55	11	88	1	45
$^2A''$(trans)	25	4	71	55	13	87	1	45

[a] Hybridization description based on GVB-PP Mulliken populations, summed over both natural orbitals of the GVB bond pair. Due to rounding to the nearest percentage and including electrons on only the metal and ligand atom directly bonded to it, percentages may not add exactly to 100%. [b] Metal atom refers to the metal atom directly bonded to the ligand. [c] The s, p, d percentages show the distribution of whatever charge is on the atom in the bonding pair in the various types of orbitals. The total percentage shows the percentage of the two electrons in the bonding pair that reside on the atom in question. [d,e] See Table 1a, footnotes *d*, *e*.

and K_{dd} are the s–d and d–d exchange terms for Zr). Hartree–Fock calculations on Zr atom predict these exchange integrals to be K_{sd} = 8.8 kcal/mol and K_{dd} = 14.0 kcal/mol. This means the exchange loss for the complexes will be 13.2 and 7.0 kcal/mol, respectively, for quartet and doublet state complexes, assuming either pure s or pure d bonding, respectively. Refinements of this exchange loss model which weight the different exchange losses for these two bonding patterns by the actual percentages of d and s character in the bonding orbital in each state were not found to change these conclusions significantly. Thus we applied the crude pure s or pure d bonding corrections to the diabatic bond energies in order to obtain estimated intrinsic bond energies.

Upon examintion of Table 7, we can see immediately that the quartet states generally have higher intrinsic bond strengths than doublet states, by as much as ~20 kcal/mol. It is also apparent (in Table 6a) that the inclusion of the extra diffuse function in basis 2 does not significantly affect these trends. The differences between the predicted bond strengths are less than 0.8 kcal/mol, and these differences do not affect the relative trends among the states' bond strengths. The sd hybrid (33–55% s character) bonds of the quartet states are much stronger than the d orbital (10% s character) bonds formed by the doublet states. The greater strength of TM sd hybrid versus pure d bonds to ligands has also been observed by Schilling et al.[31] The stronger bonds, however, are nearly offset by larger exchange losses for the quartet states: the difference between the strongest doublet, $^2\Delta$, and strongest quartet state, $^4\Sigma^-$, bond energies decreases from 11.0 kcal/mol intrinsically to 4.8 kcal/mol diabatically. Finally, when the promotional cost of 14.2 kcal/mol is included for the quartet states in the adiabatic bond strengths, the doublet bond strengths are seen to be much stronger. The strongest doublet bond, for $^2\Delta$ at 51.1 kcal/mol, is 9.4 kcal/mol stronger than the strongest quartet bond (for $^4\Sigma^-$). Thus, the higher intrinsic strength obtained by forming sd hybrid bonds is more than offset by the exchange losses and promotional costs incurred in going to the ^{5}F atomic state of Zr. Thus the preference for Zr–ligand bonding is toward nearly pure d-electron bonding. This trend holds true generally for the monometallic Zr methyls as well.

Among the four states of $ZrCH_3$ investigated, the quartet state intrinsic Zr–C bond strengths are much larger than those of the

TABLE 6

(a) Bond Energies (kcal/mol) for Zr and Pt Hydrides

bond[a]	GVB-PP[b]	RCI[b]	CCCI[b] diabatic[c]	CCCI adiabatic[c]
Zr–H basis 1[d]				
$^4\Delta$	29.1	29.7	36.8	22.6
$^2\Sigma^+$	5.4	5.4	41.7	41.7
$^4\Pi$	20.5	20.8	48.6	34.4
$^4\Sigma^-(\pi\bar{\pi}\sigma)$	42.7	43.0	50.8	36.6
$^2\Pi$	34.4	34.7	45.7	45.7
$^4\Sigma^-(\delta\bar{\delta}\sigma)$	47.4	47.6	55.9	41.7
$^2\Delta$	41.9	42.1	51.1	51.1
Zr–H basis 2[d]				
$^4\Delta$	29.1	29.7	36.6	22.4
$^2\Sigma^+$	5.4	5.5	41.7	41.7
$^4\Pi$	20.5	20.9	48.5	34.3
$^2\Pi$	34.5	34.7	45.9	45.9
$^4\Sigma^-(\pi\bar{\pi}\sigma)$	42.7	43.0	51.6	37.4
$^4\Sigma^-(\delta\bar{\delta}\sigma)$	47.4	47.6	55.9	41.7
$^2\Delta$	42.0	42.1	51.9	51.9
PtZr–H RECP 1[e]				
$^2A'$	58.6	57.3	65.4	65.4
Pt–H RECP 1				
$^2\Pi$	35.3	36.0	47.7	47.7
$^2\Sigma^+$	48.9	50.2	63.8	63.8
$^2\Delta$	50.5	50.5	63.9	63.9
Pt–H RECP 2[e]				
$^2\Pi$	45.8	46.2	58.1	58.1
$^2\Sigma^+$	56.1	57.3	70.8	70.8
$^2\Delta$	60.4	60.5	73.6	73.6
ZrPt–H RECP 1				
$^2A''$	51.1	59.1	71.5	71.5

(b) Bond Energies (kcal/mol) for Zr and Pt Methyls

$Zr–CH_3$ basis 1[d]				
$^4A'$	40.6	40.8	56.1	41.9
$^2A'$	37.8	38.0	52.0	52.0
$^2A''$	36.9	37.0	52.5	52.5
$^4A''$	45.3	45.5	60.7	46.5
$PtZr–CH_3$ RECP 1[e]				
$^2A'$(cis)	46.9	44.6	55.7	55.7
$^2A'$(trans)	47.7	45.5	56.6	56.6
$Pt–CH_3$ RECP 1				
^2E	36.4	36.4	51.6	51.6
$ZrPt–CH_3$ RECP 1				
$^2A''$(cis)	33.5	41.3	54.5	54.5
$^2A''$(trans)	35.9	44.3	57.3	57.3

[a] See Table 3a, footnote *a*. [b] See Table 1, footnote *b*. [c] Diabatic refers to the dissociation pathway for a molecule in which the fragments are not allowed to relax electronically (e.g., $^4A''$ $ZrCH_3$ dissociating into ^5F Zr even though the ^3F Zr is the ground atomic state). Geometric relaxation is allowed to take effect in this diabatic pathway. Adiabatic pathways allow both geometric and electronic relaxation of fragments to occur. [d,e] See Table 1a, footnotes *d*, *e*.

doublet states, by 10–15 kcal/mol, similar to the monometallic Zr hydrides. However, the larger exchange loss for the quartet again decreases the difference in bond strengths between the strongest quartet bond, $^4A''$ (60.7 kcal/mol), and the strongest doublet bond, $^2A''$ (52.5 kcal/mol), to 8 kcal/mol diabatically. And finally, the $^2A''$ bond energy is the largest for $ZrCH_3$ adiabatically at 52.5 kcal/mol, since the promotional cost weakens the $^4A''$ diabatic bond strength by 14.2 kcal/mol. Thus again, the promotional and exchange energy losses are more significant than the inherently stronger sd hybrid bonds of the quartet states. We now move on to comparing Pt and Zr bond strengths.

For the Pt hydrides (Table 6a), we see a consistent difference between the predictions of the two RECP's: the 18-electron RECP predicts bond energies ~10 kcal/mol larger than the 10-electron RECP. Thus, we realize that by using RECP 1, we are probably underestimating the bond strengths of Pt-bonded species. We consider here only the lower limits on the Pt–X bond strengths given by RECP 1. Diabatically, the strongest PtH bond ($^2\Delta$ at 63.9 kcal/mol) is 8 kcal/mol stronger than the strongest ZrH bond ($^4\Sigma^-$, at 55.9 kcal/mol). The adiabatic bond strengths only

TABLE 7: Intrinsic, Diabatic, and Adiabatic Energies (kcal/mol) for Monometallic Zr Hydrides and Methyls

bond[a]	CCCI[b] intrinsic[c]	CCCI diabatic[d]	CCCI adiabatic[d]
Zr–H basis 1[e]			
$^4\Delta$	50.0	36.8	22.6
$^2\Sigma^+$	48.7	41.7	41.7
$^4\Pi$	61.8	48.6	34.4
$^4\Sigma^-(\pi\bar{\pi}\sigma)$	64.0	50.8	36.6
$^2\Pi$	52.7	45.7	45.7
$^4\Sigma^-(\delta\bar{\delta}\sigma)$	69.1	55.9	41.7
$^2\Delta$	58.1	51.1	51.1
$Zr–CH_3$ basis 1[e]			
$^4A'$	69.3	56.1	41.9
$^2A'$	59.0	52.0	52.0
$^2A''$	59.5	52.5	52.5
$^4A''$	73.9	60.7	46.5

[a,b,d,e] See Table 6a for explanations. [c] Intrinsic bond strength refers to a bond strength with exchange losses and promotional costs eliminated. See text for details.

increase this difference, where the bond strength of $^2\Delta$ PtH is 12 kcal/mol larger than the strongest ZrH bond, $^2\Delta$, due to the greater metal sd hybrid character present in the Pt–H bond compared to the ZrH bond (primarily metal d). Overall, the low spin $Pt–CH_3$ and $Zr–CH_3$ adiabatic bond strengths (Table 6b) are the largest and are essentially equivalent at approximately 52 kcal/mol. Intrinsically, the quartet $ZrCH_3$ bonds have more s character, are more ionic, and are ~22 kcal/mol stronger than that of $PtCH_3$, but promotional costs ultimately offset this inherent advantage.

Comparison of our calculated bond energies for the monometallic complexes to those of previous studies shows general agreement. The adiabatic bond energy (allowing electronic and geometric relaxation in the fragments) calculated for the ground state of ZrH (51.1 kcal/mol) is close to that given by Langhoff et al.[18] (53.5–55.4 kcal/mol). The M–C bond energies for the $^2A'$ and $^2A''$ states of $ZrCH_3$ (52.0–52.5 kcal/mol) compare favorably to the M–C bond energy predicted for the ^2E state (51.3–53.3 kcal/mol) by Bauschlicher et al.[17] Our predicted values for the $^2\Sigma^+$ PtH bond strength of 63.8 kcal/mol (RECP 1) and 70.8 kcal/mol (RECP 2) fit comfortably within the range of theoretical predictions (59.3–75.4 kcal/mol) from varied sources.[9,10,12] The same holds true for our predicted $^2\Delta$ PtH bond strengh: the range of previously predicted values, 57.9–79.1 kcal/mol,[8–10,12] and the experimental prediction[14] of <80 kcal/mol bracket our values of 63.9 kcal/mol (RECP 1) and 73.6 kcal/mol (RECP 2). Note that, despite the difference in bond strength predictions of the two RECPs, neither theoretical nor experimental studies provide a basis for differentiating between the two. We will therefore use the more economical 10-electron RECP for the diatomic studies with the caveat that our Pt-bonded species bond strengths may be underestimated. Thus all our predicted bond energies compare well with available literature precedents and lend credence to the expectation that our bimetallic bond strengths will also be fairly accurate.

In the metal diatomic–ligand complexes, the Zr-bonded species no longer have any promotional cost to pay and thus the trends mirror those of the diabatic bond strengths of their low-spin monometallic analogs. For example, one can see from Table 6b that the $PtZr–CH_3$ and $ZrPt–CH_3$ bond strengths are very similar, 55.7 and 54.5 kcal/mol for the cis conformers and 56.6 and 57.3 kcal/mol for the trans conformers, respectively. The Zr-bonded species' metal diatomic–ligand bond is slightly stronger among the two cis conformers, as in the low-spin monometallic species, whereas the Pt-bonded trans conformer has the strongest metal diatomic–methyl bond of all the metal diatomic–methyl complexes. This shows that the metal diatomic-ligand bond strengths are all quite similar throughout the metal diatomic–methyl complexes and that the difference in the metal diatomic–ligand

stabilities between the Pt- and Zr-bonded complexes is of the same order as a rotational barrier of the methyl group. The metal diatomic hydride bond strengths (Table 6a) also follow the monometallic trends qualitatively, with the Pt-bonded species having an approximately 6 kcal/mol stronger bond than the Zr-bonded species. ZrPtH has the strongest bond of all the metal diatomic–ligand species at 71.5 kcal/mol. Most importantly, both bimetallic hydride species' adiabatic bond strengths increase by an average of approximately 10 kcal/mol, relative to the monometallic species, whereas the metal diatomic methyl species' bond strengths increase by an average of only 5 kcal/mol (comparing the most strongly bound state for each case).

Summary and Implications

Zr is found to act as an electron donor in all the metal diatomic complexes. This is in accord qualitatively with the conclusions reached by Wang and Carter[2] in their higher level treatments of the ZrPt diatomic. Thus the ZrPt diatomic moiety may be thought of as $Zr^{x+}Pt^{x-}$, with $x \sim 0.5$ when a ligand binds to Pt and $x \sim 1.0$ when a ligand binds to Zr. Charge transfer is enhanced in the latter case in order to maximize s–d hybridization on Zr, which leads to stronger bonds. The Zr–CH_3 and Zr–H bonds are found to be quite polar, with bond strengths of ~52 kcal/mol. The strengths of these bonds are increased by "alloy" formation: the methyl–Zr bond only slightly (~4 kcal/mol) and the hydride–Zr bond much more (~14 kcal/mol). By contrast, the platinum–hydride and –methyl bonds are both found to be fairly covalent, with bond strengths of 64 and 52 kcal/mol, respectively. The strengths of both bonds also increase upon "alloy" formation: the methyl–Pt bond by ~6 kcal/mol and the hydride–Pt bond by ~8 kcal/mol. Thus, all the metal–ligand bond strengths are augmented in the alloy, but the metal–hybride bond strengths are increased by approximately double the change in the analogous metal–methyl bond strengths on average. Test calculations explicitly treating the outer core electrons on Pt within Pt–H indicate that the absolute Pt–H bond strength may be as much as 10 kcal/mol greater than 64 kcal/mol. However, we expect the *differences* in M–H bond strengths between the mono- and bimetallic complexes to be well represented by the above predictions using a valence-only description of Pt, even though the absolute value for the ZrPt–X bond strength may be higher than that reported here. Thus the D_e(ZrPt–X) values predicted here may be considered as lower bounds to the true D_e(ZrPt–X).

Finally, the "alloy"-induced alteration in M–H and M–CH_3 thermochemistry may have important implications for catalytic reactions involving hydrocarbons. The larger average relative increase in the metal–hydride bond strengths might favor greater hydrogen retention by a PtZr alloy surface without altering the average metal–carbon binding energies very much. This suggests that PtZr alloy surfaces might be good candidates for selective dehydrogenation of hydrocarbons, due to the increased driving force for C–H bond cleavage coupled with the small change in the stability of the subsequently formed hydrocarbon fragments on the surface. Thus little or no increase in carbidization of the surface is expected, while a possible increase in the rate of dehydrogenation compared to the rate of hydrogenolysis might be achieved.

Acknowledgment. We are grateful to the Air Force Office of Scientific Research for support of this work. E.A.C. also acknowledges support from the National Science Foundation, the Camille and Henry Dreyfus Foundation, and the Alfred P. Sloan Foundation for a Presidential Young Investigator Award, a Teacher–Scholar Award, and a Research Fellowship, respectively. G.G.R. is a National Science Foundation Predoctoral Fellow. We also wish to thank Hua Wang, who participated in the initial stages of this work, and Todd J. Martinez for many insightful conversations and helpful suggestions.

References and Notes

(1) (a) Engel, N. *Acta Metall.* **1967**, *15*, 557. (b) Brewer, L. *Acta Metall.* **1967**, *15*, 553. (c) Brewer, L. *Science* **1968**, *16*, 115.
(2) Wang, H.; Carter, E. A. *J. Am. Chem. Soc.* **1993**, *115*, 2357.
(3) Fisher, R. F.; Alvey, M. A.; George, P. M. *Aerojet Rep.* **1991**, 9784.
(4) Martinho Simoes, J. A.; Beauchamp, J. L. *Chem. Rev.* **1990**, *90*, 629.
(5) Basch, H.; Topiol, S. *J. Chem. Phys.* **1979**, *71*, 802.
(6) Basch, H.; Newton, M. D.; Jafri, J.; Moskowitz, J. W.; Topiol, S. *J. Chem. Phys.* **1978**, *68*, 4005.
(7) (a) Kahn, L. R.; Baybutt, P.; Truhlar, D. G. *J. Chem. Phys.* **1976**, *65*, 3826. (b) Hay, P. J.; Wadt, W. R.; Kahn, L. R. *J. Chem. Phys.* **1978**, *68*, 3059.
(8) Low, J. J.; Goddard, W. A., III *J. Am. Chem. Soc.* **1984**, *106*, 6928.
(9) Poulain, E.; Garcia-Prieto, J.; Ruiz, M. E. *Int. J. Quantum Chem.* **1986**, *29*, 1181.
(10) Rohlfing, C. M.; Hay, P. J.; Martin, R. L. *J. Chem. Phys.* **1986**, *85*, 1447.
(11) Hay, P. J.; Wadt, W. R. *J. Chem. Phys.* **1985**, *82*, 270, 284, 299.
(12) Tobish, S.; Rasch, G. *Chem. Phys. Lett.* **1990**, *166*, 311.
(13) Langhoff, S. R.; Davidson, E. R. *Int. J. Quantum Chem.* **1974**, *8*, 61.
(14) Huber, K.; Herzberg, G. *Constants of Diatomic Molecules*; Van Nostrand Reinhold Co.: New York, 1979.
(15) (a) Scullman, R. *Ark. Fys.* **1965**, *28*, 255. (b) Kaving, B.; Scullman, R. *Phys. Scr.* **1974**, *9*, 33.
(16) Dyall, K. G. *J. Chem. Phys.* **1993**, *98*, 9678.
(17) Bauschlicher, C. W., Jr.; Langhoff, S. R.; Partridge, H.; Barnes, L. A. *J. Chem. Phys.* **1989**, *91*, 2399.
(18) Langhoff, S. R.; Bauschlicher, C. W., Jr.; Pettersson, L. G. M.; Partridge, H. *J. Chem. Phys.* **1987**, *86*, 268.
(19) (a) Chong, D. P.; Langhoff, S. R. *J. Chem. Phys.* **1986**, *84*, 5606. (b) Alrichs, R.; Scharf, P.; Ehrhardt, C. *J. Chem. Phys.* **1985**, *82*, 890.
(20) (a) Yaffe, L. G.; Goddard, W. A., III *Phys. Rev. A* **1976**, *13*, 1682. (b) Roos, B. O. In *Ab initio Methods in Quantum Chemistry*; Lawley, K. P., Ed.; Wiley: New York, 1987; p 2.
(21) Bair, R. A.; Goddard, W. A., III; Voter, A. F.; Rappé, L. G.; Yaffe, L. G.; Bobrowicz, F. W.; Wadt, W. R.; Hay, P. J.; Hunt, W. J. *gvb2p5* program, unpublished. See: (a) Blair, R. A. Ph.D. Thesis, California Institute of Technology, 1980. (b) Bobrowicz, F. W.; Goddard, W. A., III In *Methods of Electronic Structure Theory*; Schaefer, H. F., Ed.; Plenum: New York, 1977; pp 77–129. (c) Hunt, W. J.; Hay, P. J.; Goddard, W. A., III *J. Chem. Phys.* **1972**, *57*, 738.
(22) Details about GVB can be found in the following: (a) Hunt, W. J.; Dunning, T. H., Jr.; Goddard, W. A., III *Chem. Phys. Lett.* **1969**, *3*, 606. (b) Goddard, W. A., III.; Dunning, T. H., Jr.; Hunt, W. J. *Chem. Phys. Lett.* **1969**, *4*, 231. (c) Hunt, W. J.; Goddard, W. A., III; Dunning, T. H., Jr. *Chem. Phys. Lett.* **1970**, *6*, 147.
(23) Carter, E. A.; Goddard, W. A., III *J. Chem. Phys.* **1988**, *88*, 1752.
(24) Carter, E. A.; Goddard, W. A., III *J. Chem. Phys.* **1988**, *88*, 3132.
(25) (a) Wu, C. J.; Carter, E. A. *J. Phys. Chem.* **1991**, *95*, 8352. (b) Schilling, J. B.; Goddard, W. A., III; Beauchamp, J. L. *J. Am. Chem. Soc.* **1987**, *109*, 5573. (c) Carter, E. A.; Goddard, W. A., III *J. Phys. Chem.* **1984**, *88*, 1485. (d) Carter, E. A.; Goddard, W. A., III *J. Am. Chem. Soc.* **1988**, *110*, 4077.
(26) Smith, G. W.; Carter, E. A. *J. Phys. Chem.* **1991**, *95*, 2327, 10828.
(27) (a) Dunning, T. H., Jr. *J. Chem. Phys.* **1970**, *53*, 2823. (b) Huzinaga, S. *J. Chem. Phys.* **1965**, *42*, 1293.
(28) (a) Schlegel, H. B. *J. Comput. Chem.* **1982**, *3*, 214. (b) Dupuis, M.; King, H. F. *J. Chem. Phys.* **1978**, *68*, 3998.
(29) Moore, C. E. *Atomic Energy Levels As Derived From the Analyses of Optical Spectra*; U.S. Government Printing Office: Washington, DC, 1971; Vol. III, pp 38–43, 181–185.
(30) Carter, E. A.; Goddard, W. A., III *J. Phys. Chem.* **1988**, *92*, 5679.
(31) Shilling, J. B.; Goddard, W. A., III; Beauchamp, J. L. *J. Am. Chem. Soc.* **1987**, *109*, 5565.